OCB identification and reconnection voltage estimate using FUV imaging

Benoit HUBERT
LPAP, University of Liège, Belgium

B.Hubert@ulg.ac.be

IMAGE-FUV instruments

- The IMAGE-FUV imaging instruments included
  - WIC (Wide band Imaging Camera) (N_2 LBH domain: ~1300 – 1900 Å)
  - SI13 (Spectrographic Imaging at 1356 Å): OI 1356 line
  - SI12 (Spectrographic Imaging at 1218 Å): HI Doppler-shifted Lyman-α auroral emission.

IMAGE FUV instruments

- ULg was included in the IMAGE-FUV experiment from the very beginning:
  - Manufacturing of the SI instrument
  - Modelling of the aurora and estimate of the instrument response (count – Rayleigh conversion) in collaboration with our Russian colleagues.

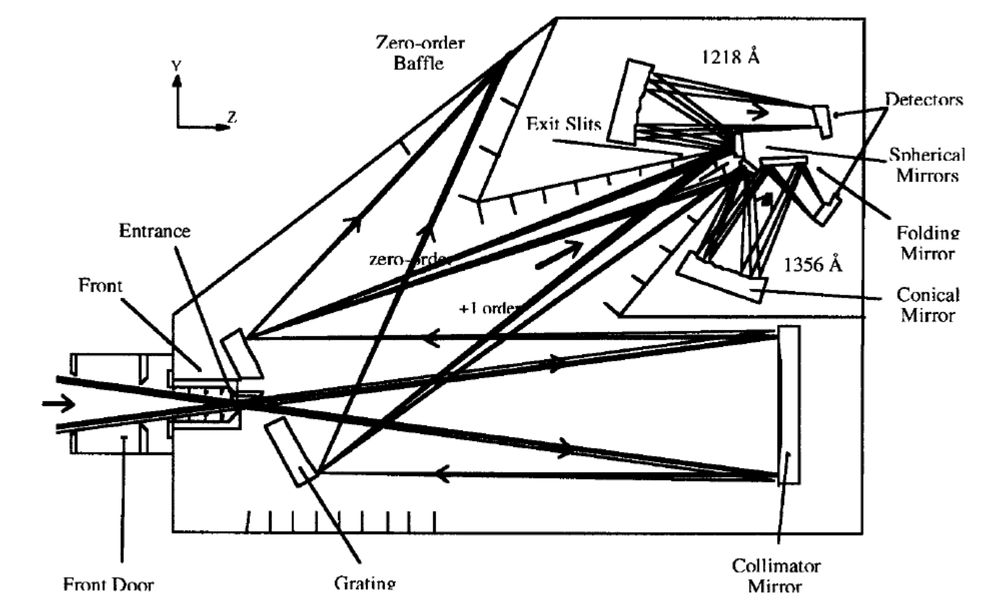

Figure 3. The IMAGE Spectrographic Imager schematic.

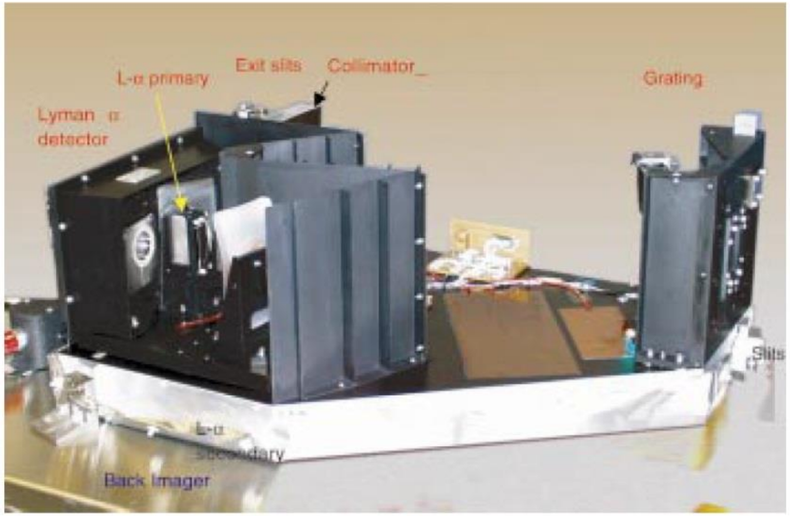

Figure 4. The Spectrographic Imager without its cover.

IMAGE-FUV instruments

- Efficiency curves for WIC, SI13 and SI12 were obtained depending on the characteristic energy of the precipitating particles

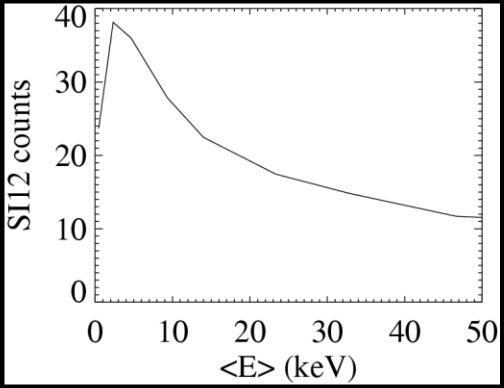

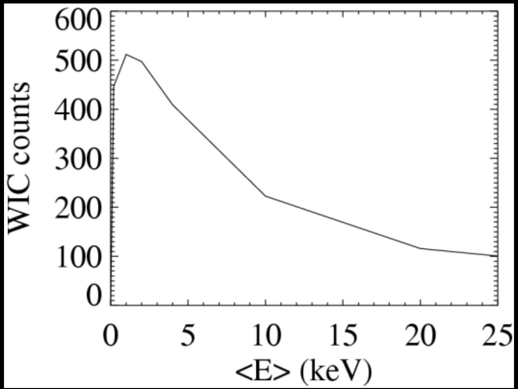

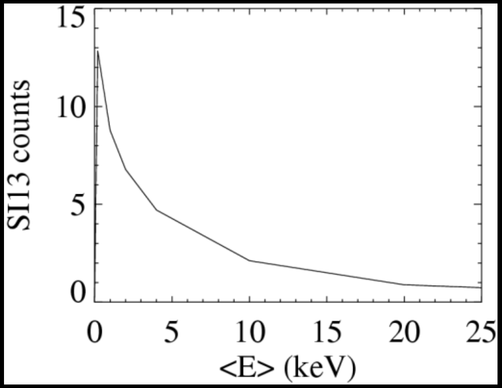

Allows calculation of the proton energy flux from the SI12 measurements, at the expense of an assumption on $\langle E_p \rangle$. Similar curves have been calculated for the proton aurora contribution to WIC and SI13.

Allows calculation of the electron average energy and energy flux from the WIC and SI13 measurements, after having removed the proton aurora contribution to these signals.

Hemispheric power estimate

- Efficiencies could be used to estimate the auroral energy input in the ionosphere.

December 25, 2000

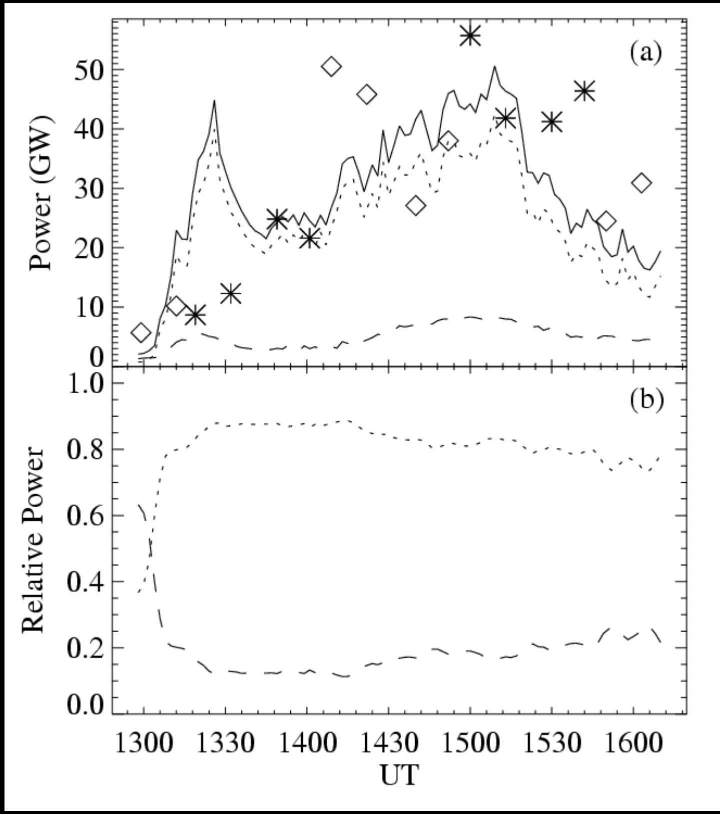

December 9, 2000

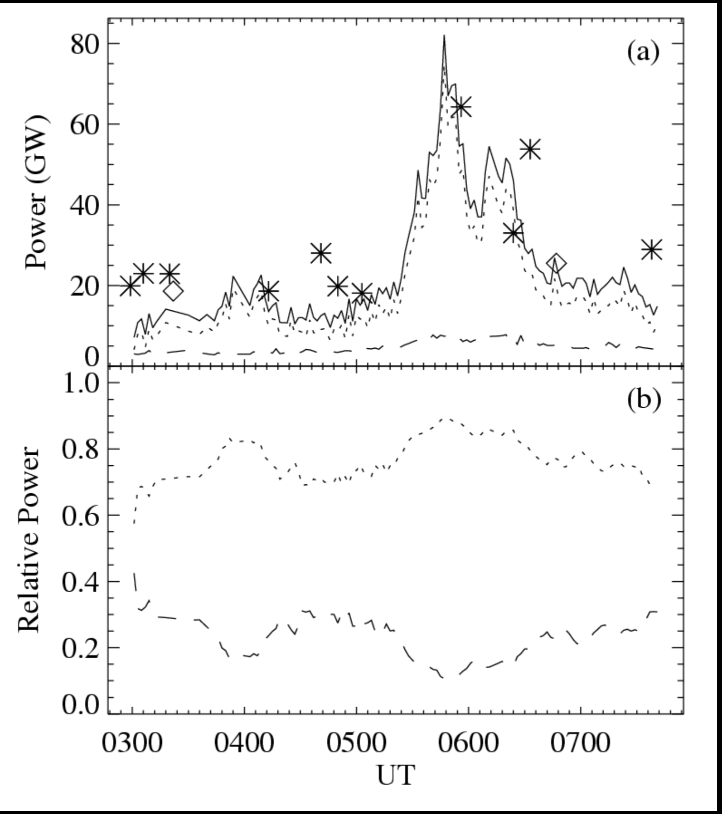

Auroral morphology studies

- Quantitative analysis can be performed based on imaging, especially when several wavelengths are observed.
- The Monte Carlo model simulating the proton (and later the electron) aurora can be upgraded to compute the upward flux of particles.
- Morphology of the aurora can be used in several manner: identification of special signatures (transpolar aurora, for example), or determination of the state of the magnetosphere at the global scale (open magnetic flux and reconnection rate)

Physical framework: the Dungey cycle

- Open magnetic flux is created on the dayside when the IMF and the geomagnetic field interconnect.
- Newly opened field lines are « convected » to the nightside.
- Open flux is eventually closed in the tail when the topology of the magnetic field is reconfigured.

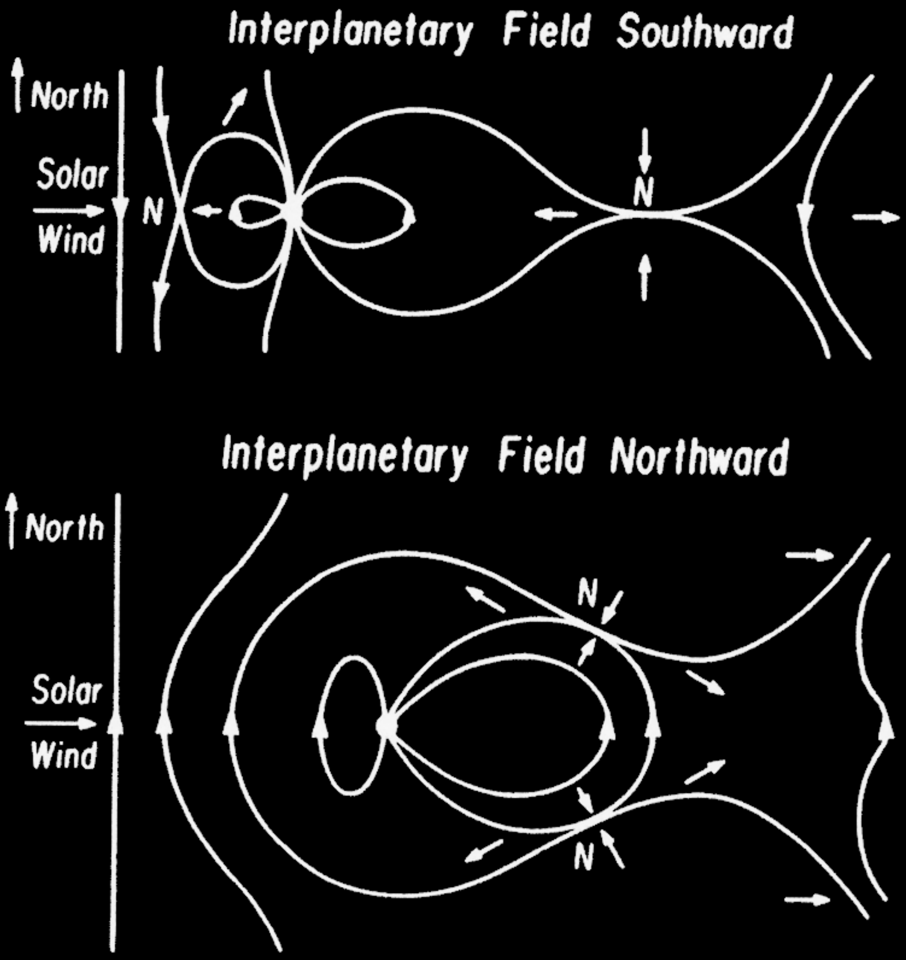

Physical framework: the Dungey cycle

- The ionospheric counterpart of the cycle of magnetic flux opening and closure is ionospheric convection and the associated ionospheric electric field and the location of the auroral emission
- Observation of the aurora and ionospheric convection can be used to diagnose magnetic reconnection and the production of open magnetic flux

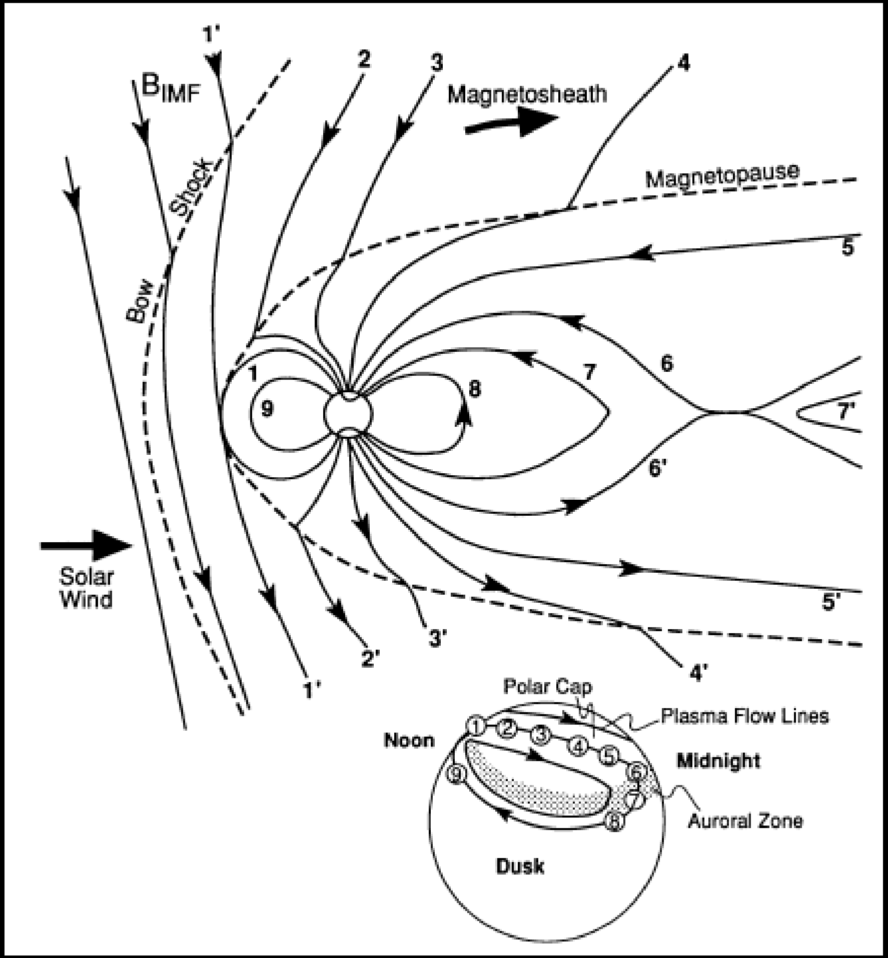

Method outline

- Use FUV imaging (previously IMAGE-SI12) to identify the OCB (open-close field line boundary) location
- Follow OCB motion (=> motional electric field)
- Use SuperDARN radar measurement of ionospheric convection (=> ionospheric electric field)
- Compute the flux threading the polar cap and the reconnection voltage near the dayside magnetopause and in the magnetotail.

Previous applications

- Substorm reconnection monitoring
- Shock-induced flux closure
- Sawtooth event monitoring
- Auroral streamer analysis
- Steady magnetospheric convection (SMC) montoring
- Magnetospheric mode classification

SI12 passband and proton aurora

- Proton aurora not contaminated by dayglow (works at all season)
- Electron aurora can be contaminated by dayglow (but the UVI passband is chosen to minimize that problem).

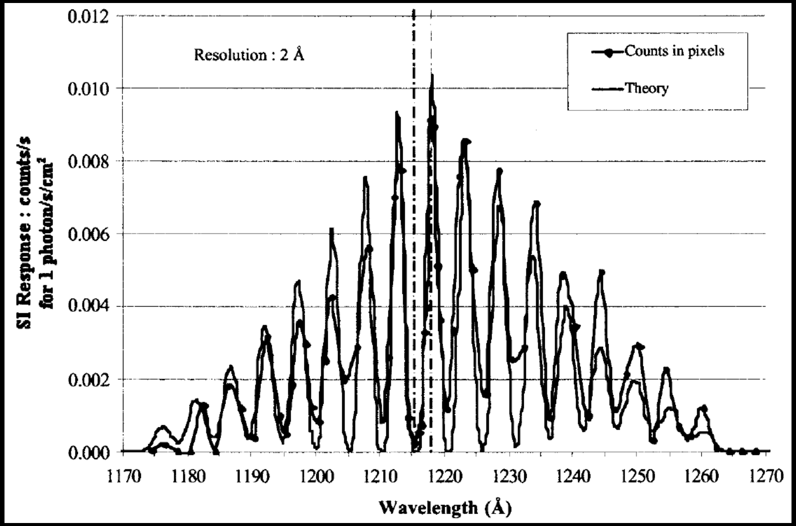

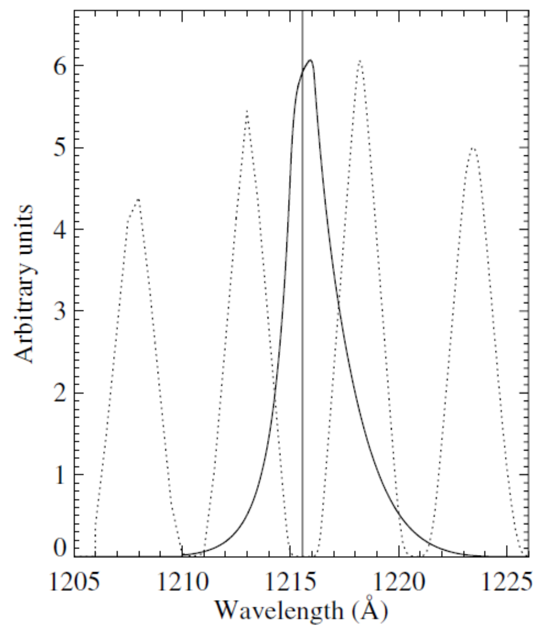

Previous SI12 applications: principles

- Magnetic flux: $\Phi = \int_S \vec{B} \cdot \vec{n}\, ds$
- Reconnection rate (Faraday): $\frac{d\Phi}{dt} = -\oint_C \vec{E} \cdot d\vec{l}$
  - Over C: net rate of change of Φ
  - Positive part: dayside flux opening
  - Negative part: nightside flux closure

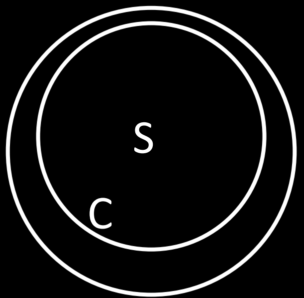

- Electric field computed in the frame of reference of the moving open/closed boundary: includes the ionospheric and the motional electric fields.

$$\vec{E} = \vec{E}_i + \vec{v} \times \vec{B}$$

Previous SI12 applications: substorms

- Boundary assimilated with the poleward edge of the proton aurora (+DMSP correction)
  - SI12 preferred for absence of dayglow contamination
  - fitted with a Fourier series
  - Motion determined after time smoothing
  - Motional electric field is computed

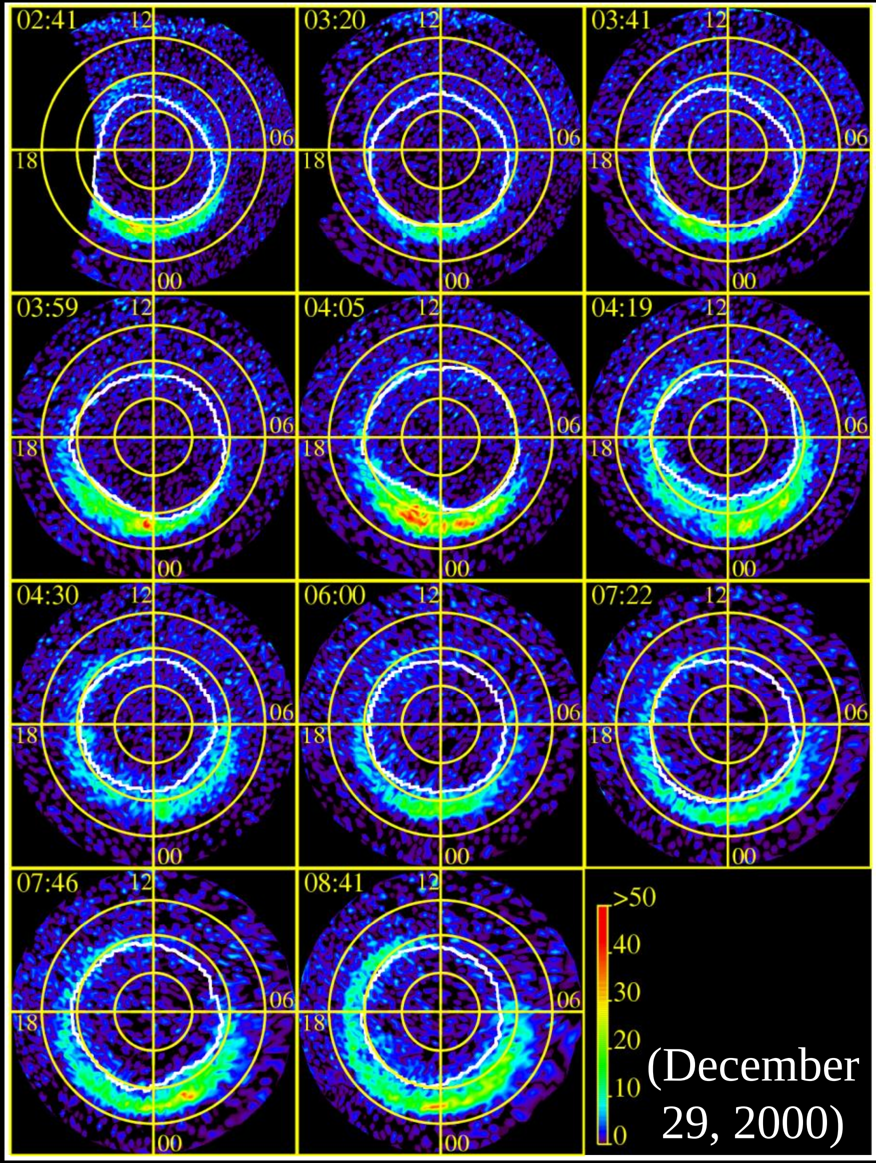

Previous SI12 applications: substorms

- The convection flow pattern is retrieved from the SuperDARN echoes
- Shows how open and reconnected field lines evolve
- The ionospheric potential is retrieved using the Map-Potential technique [*Ruohoniemi and Baker,* 1998]

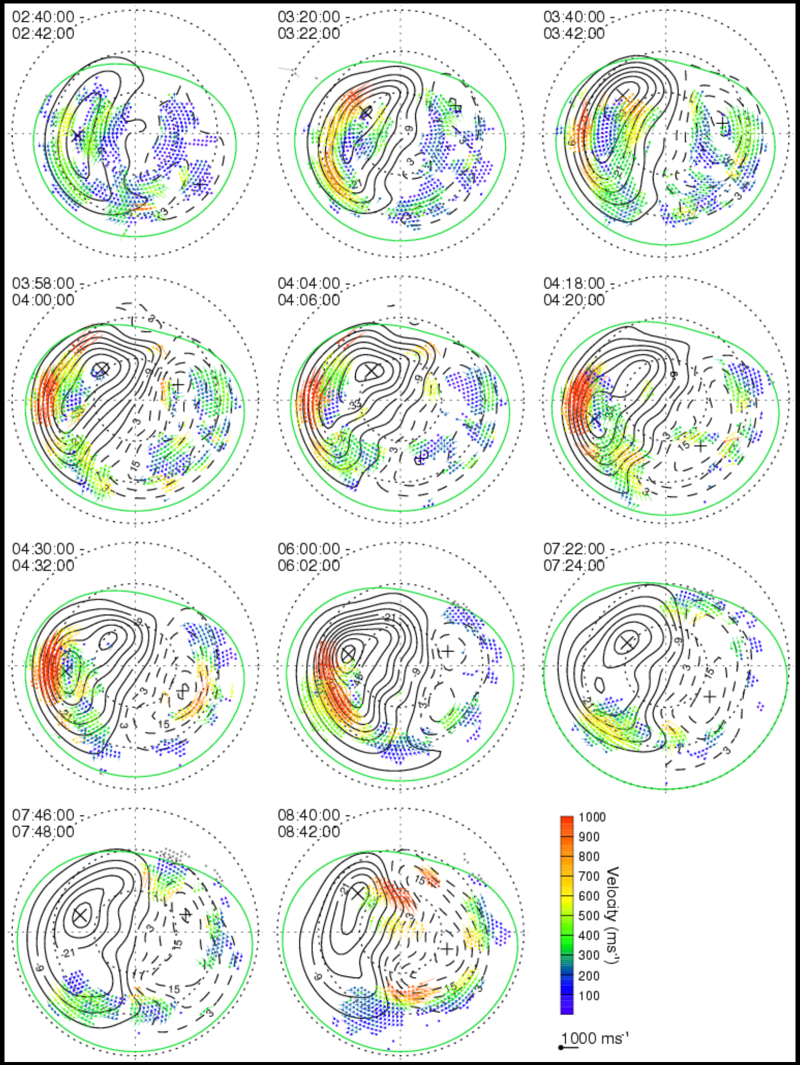

Previous SI12 applications: substorms

- IMF B_z (WIND) is southward ~throughout the interval

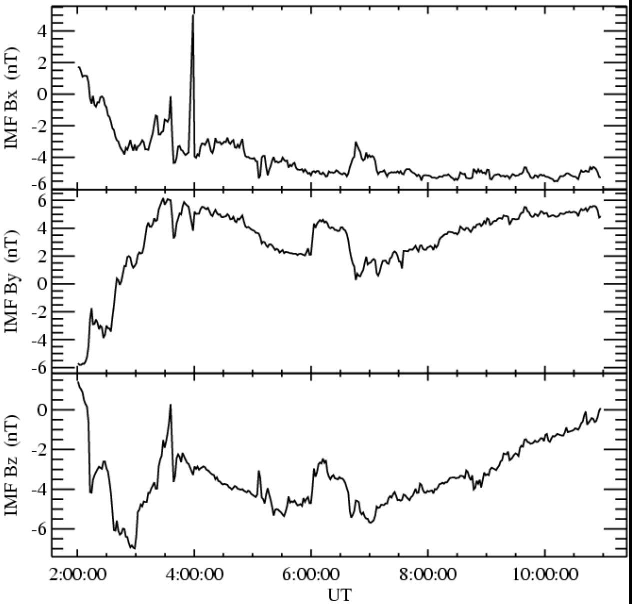

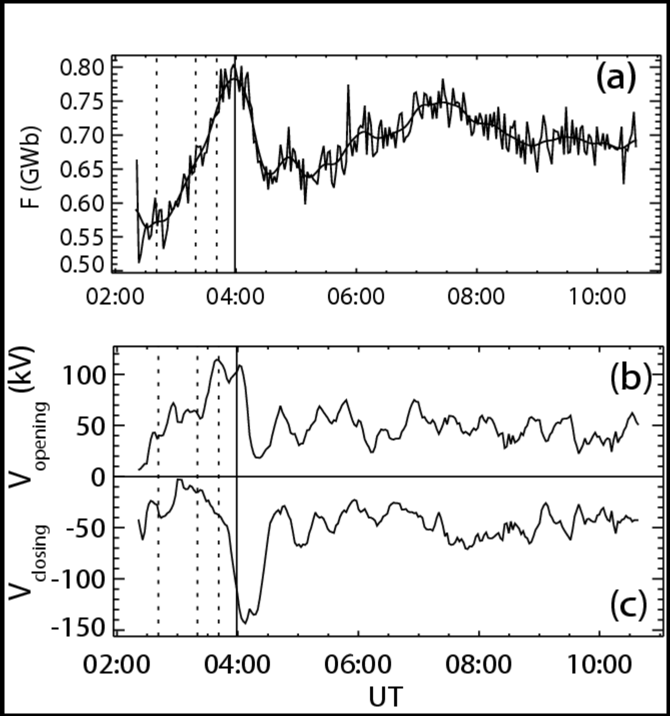

- Pseudobreakups (dotted vertical line) close flux prior to onset (solid vertical line)
- Maximum flux closure rate shortly after onset (100 – 150 kV)
- Enhancement of PBI brightness related to progressive enhancement of flux closure voltage
- Quiet time closure voltage ~30 kV

Previous SI12 applications: shocks

- 2 solar wind density discontinuities caused DSPF's [Hubert et al., 2003] on 8 November 2000
- B_z northward ⇒ no open flux accumulation, no substorm expansion
- Intense flux closure when the shocks interact with the tail

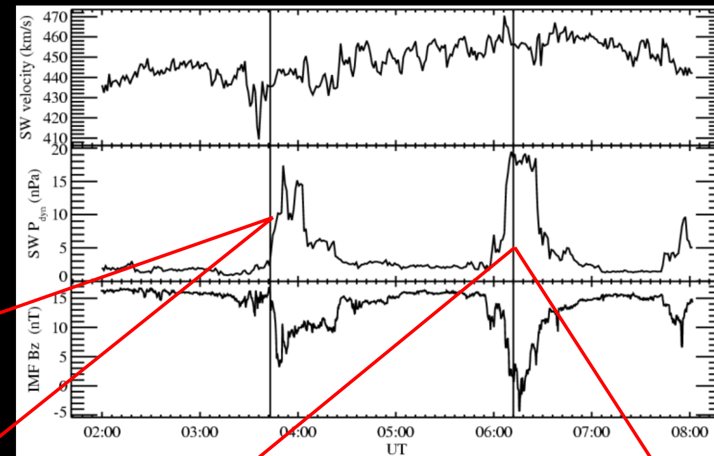

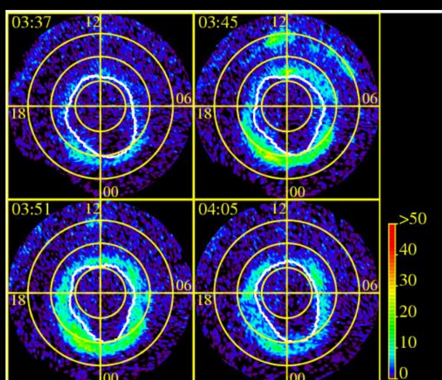

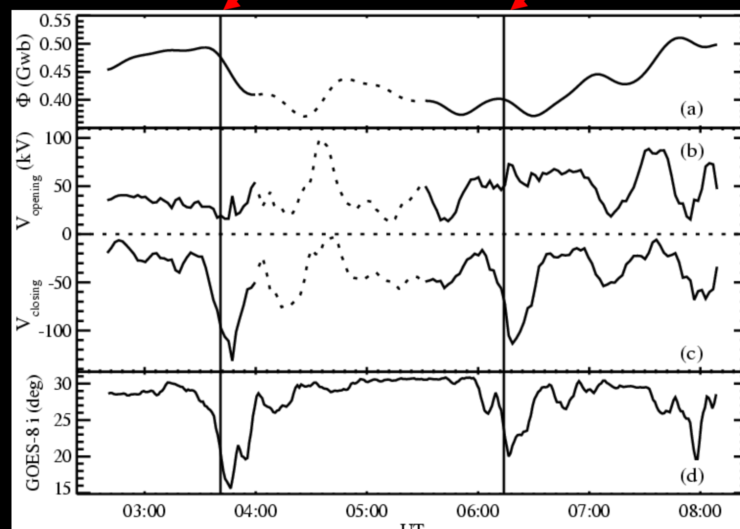

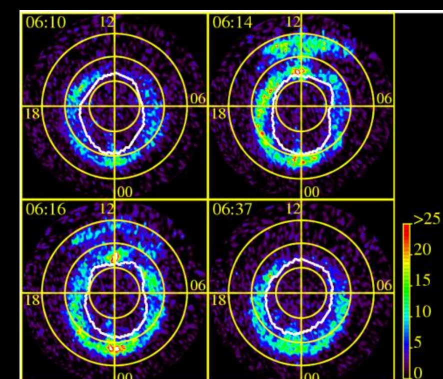

Statistics: ΔP_{dyn}~2.8 nPa (over time scales of a few minutes) discriminates between weak and strong shocks, i.e. preconditioning vs shock-driven flux closure.

Previous SI12 applications: modes

Compared quiet times, substorms, steady magnetospheric convection intervals and sawtooth events

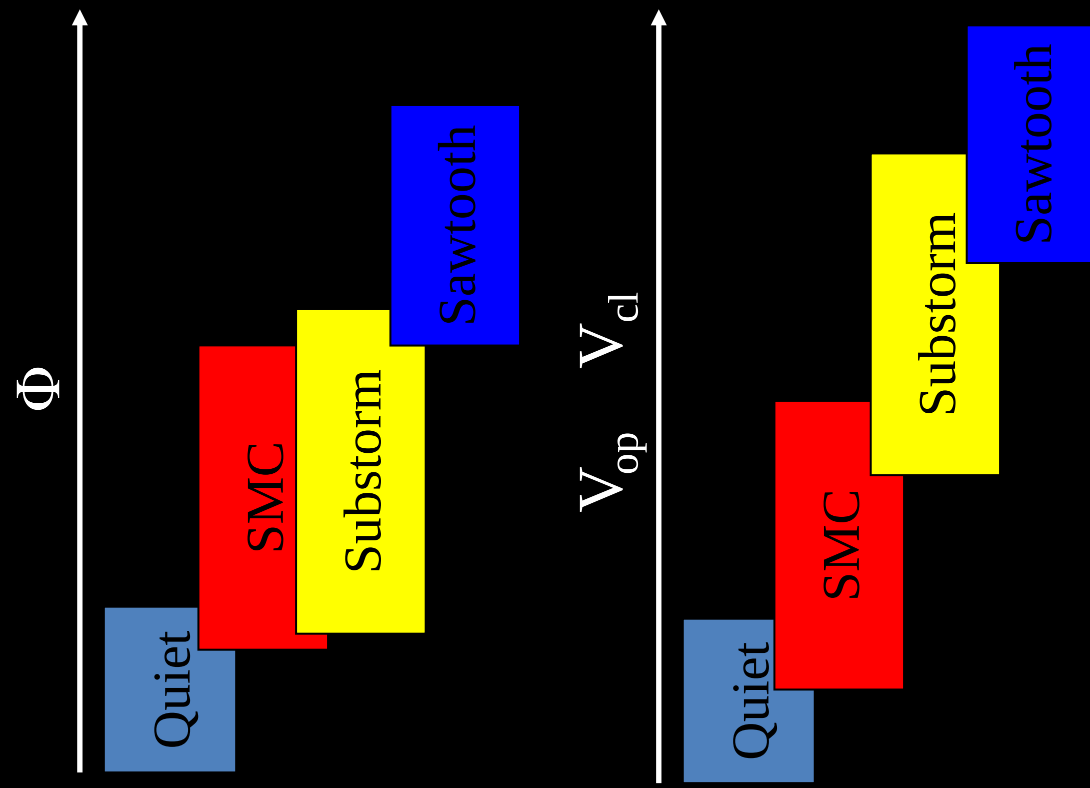

	Quiet time	**SMC**	**Substorm**	**Sawtooth**
Φ (GWb)	< ~0.4 – 0.5	~0.6 – 0.9	~0.65 - 0.9 0.7 - 0.96 peak	~1.0 – 1.4
V_{op}, V_{cl} (kV)	< ~40	~35 - 75	~70 – 140 peak	~60 – 160

Future possibilities with SMILE

- FUV imaging will be complemented with
  - particles and field measurements in the solar wind
  - Imaging of the interaction at the magnetopause
    - $\Rightarrow$ Ideal for the study of shock-induced phenomena
    - $\Rightarrow$ Worth being compared with the flux opening voltage (cusp signature?)
- Orbit will offer longer imaging intervals + better cadence
  - Needed for storm studies
  - Better for long time scale processes (SMC etc.)
  - Still allow the study of short time scale phenomena
- FUV imaging passband tuned for the electron aurora
  - Good s/n ratio
  - Possible dayglow contamination in summer

Possible dayglow issues

- Near winter solstice (7 December 2000): no problem

SI13

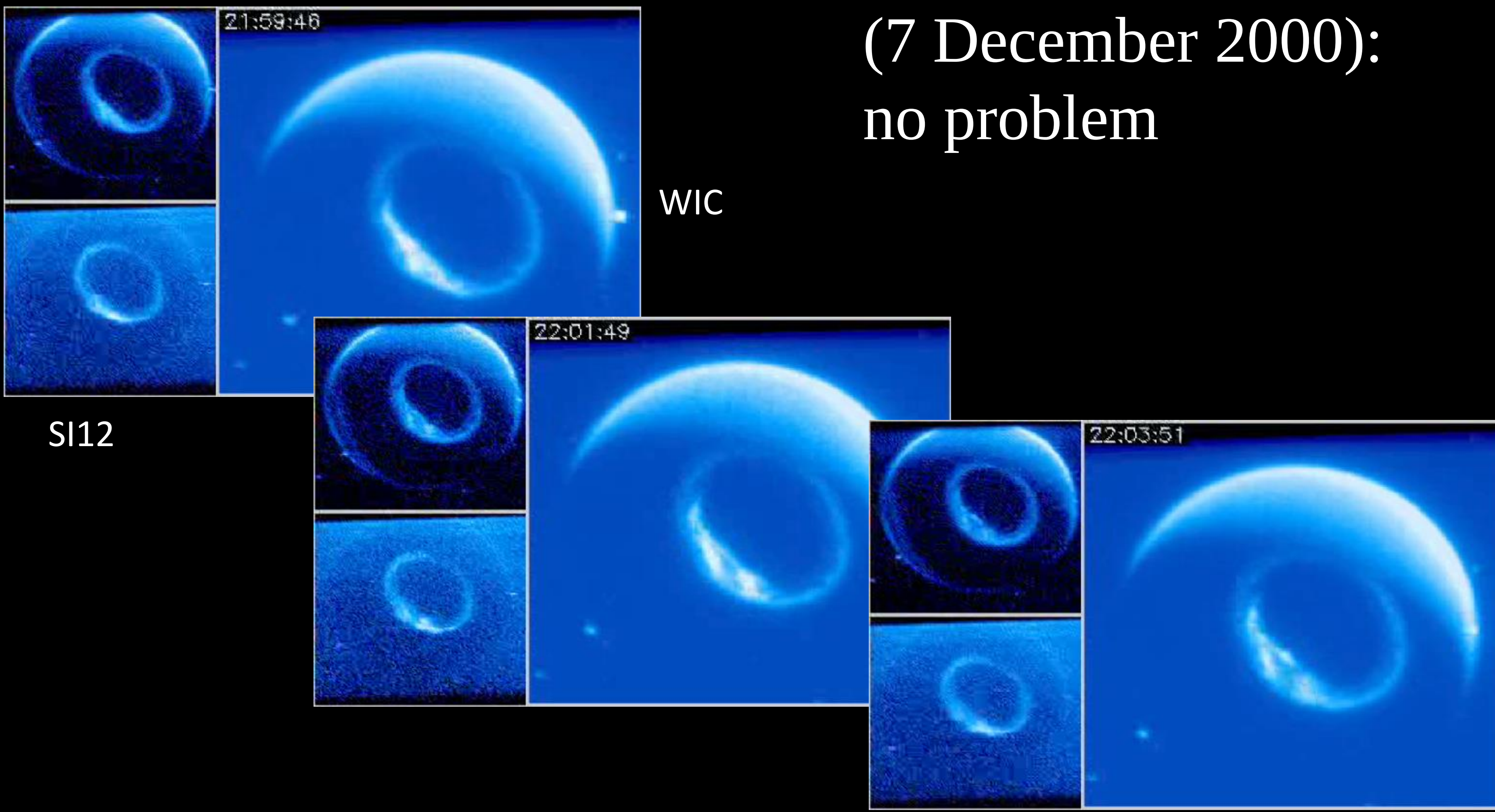

WIC

SI12

Possible dayglow issues

- Near summer solstice (1st June 2001): More difficult to identify a weak aurora on the dayside.
- Passband will reject the $\lambda > 200$ nm as much as possible

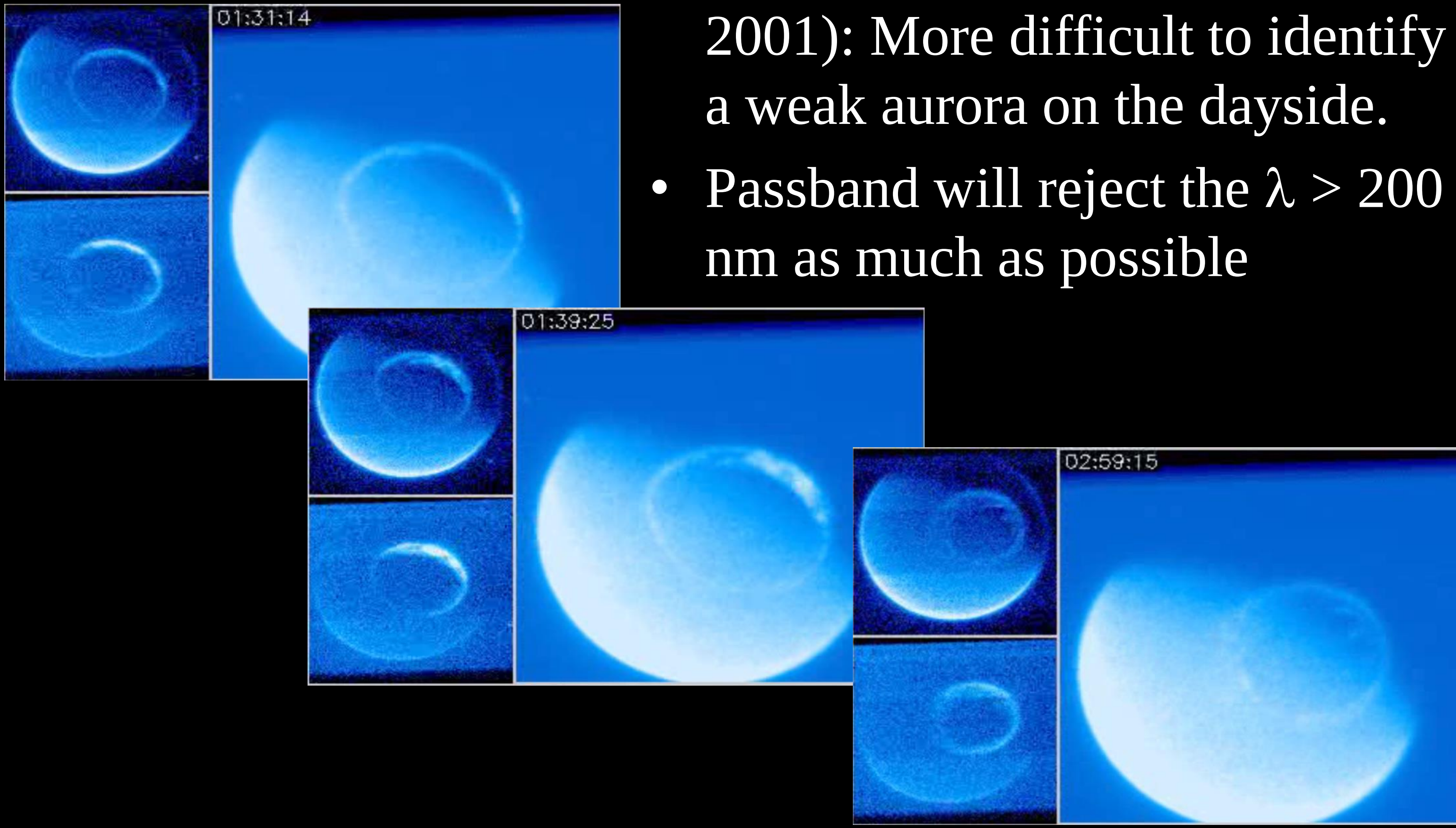

Handling the dayglow

- Tests on a difficult case: WIC images in summer
- Current method: Fourier series fitted on the non-auroral part of the image and extrapolated in the auroral region
- Improve s/n ration: group pixels (in space and time)
- Principal component analysis (Kharunen Lohève transform)
  - may seem promising at identifying the part of the image that does not change much: the dayglow
  - However, the aurora also has a contribution to the images having the largest eigenvalue
- Generalized Savitsky-Golay filter: still leaves structures hardly distinguishable of weak auroral features.

Possible dayglow issues

- Dayglow subtraction with Savitsky-Golay filtering
- A comparison with other boundary identification techniques will be necessary (i.e. DMSP)

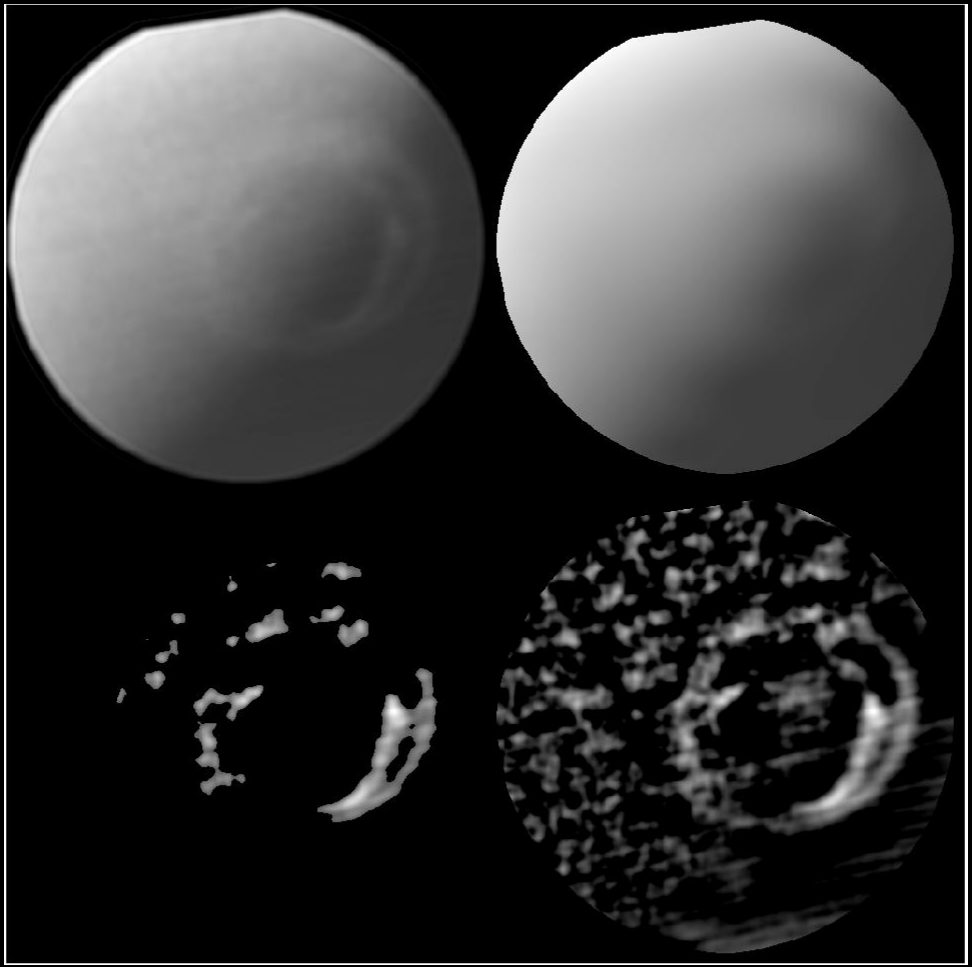

Summary

- Techniques developed for previous missions can be used for the analysis of the SMILE-UVI data, at least over a part of the year
- SMILE will
  - offer the possibility to directly relate the auroral and magnetospheric dynamics to the solar wind forcing
  - provide a better time coverage (longer sequences) with a better cadence.
- Near summer solstice, efficient dayglow subtraction will be needed to analyze weak auroral emissions (i.e. OCB identification)

References

- B. Hubert, M. Palmroth, T. V. Laitinen, P. Janhunen, S. E. Milan, A. Grocott, S. W. H. Cowley, T. Pulkkinen, and J.-C. Gérard. ”Compression of the Earth’s magnetotail by interplanetary shocks directly drives transient magnetic flux closure.” *Geophysical Research Letters* 33, no. 10 (May 31, 2006).
- B. Hubert, S. E. Milan, A. Grocott, S. W. H. Cowley, and J.-C. Gérard. ”Open magnetic flux and magnetic flux closure during sawtooth events.” *Geophysical Research Letters* 35 (December 1, 2008): 23301.
- B. Hubert, S. E. Milan, A. Grocott, C. Blockx, S. W. H. Cowley, and J.-C. Gérard. ”Dayside and nightside reconnection rates inferred from IMAGE FUV and Super Dual Auroral Radar Network data.” *Journal of Geophysical Research. Space Physics* 111, A3 (March 28, 2006).
- B. Hubert, K. Kauristie, O. Amm, S. E. Milan, A. Grocott, S. W. H. Cowley, and T. I. Pulkkinen. ”Auroral streamers and magnetic flux closure.” *Geophysical Research Letters* 34, no. 15 (August 9, 2007).
- B. Hubert, J.-C. Gérard, S. E. Milan, and S. W. H. Cowley. ”Magnetic reconnection during steady magnetospheric convection and other magnetospheric modes.” *Annales Geophysicae* 35 (March 1, 2017): 505-524.
- B. Hubert, J.-C. Gérard, S. A. Fuselier, and S. B. Mende. ”Observation of dayside subauroral proton flashes with the IMAGE-FUV imagers.” *Geophysical Research Letters* 30 (February 1, 2003): 45-1.
- B. Hubert, C. Blockx, S. E. Milan, and S. W. H. Cowley. ”Statistical properties of flux closure induced by solar wind dynamic pressure fronts.” *Journal of Geophysical Research. Space Physics* 114 (July 1, 2009): 07211.
- B. Hubert, A. T. Aikio, O. Amm, T. Pitkanen, K. Kauristie, S. E. Milan, S. W. H. Cowley, and J.-C. Gérard. ”Comparison of the open-closed field line boundary location inferred using IMAGE-FUV SI12 images and EISCAT radar observations.” *Annales Geophysicae* 28 (April 1, 2010): 883-892.
- Hubert B., Gérard, J.C., Mende S. B., Fuselier S. A., Statistical properties of Dayside Subauroral Proton Flashes observed with IMAGE-FUV, in *Inner Magnetosphere Interactions: New Perspectives From Imaging*, James L. Burch, Michael Schulz, Harlan Spence, Editors AGU Geophysical Monograph Series, Volume 15, ISBN 0-87590-424-6 9, 2005
- M. Meurant, J.-C. Gérard, B. Hubert, V. Coumans, C. Blockx, N. Ostgaard, and S. B. Mende. ”Dynamics of global scale electron and proton precipitation induced by a solar wind pressure pulse.” *Geophysical Research Letters* 30, no. 20 (October 18, 2003).
- S. E. Milan, J. S. Gosling, and B. Hubert. ”Relationship between interplanetary parameters and the magnetopause reconnection rate quantified from observations of the expanding polar cap.” *Journal of Geophysical Research. Space Physics* 117 (2012): 03226.

Auroral streamers and BBF’s

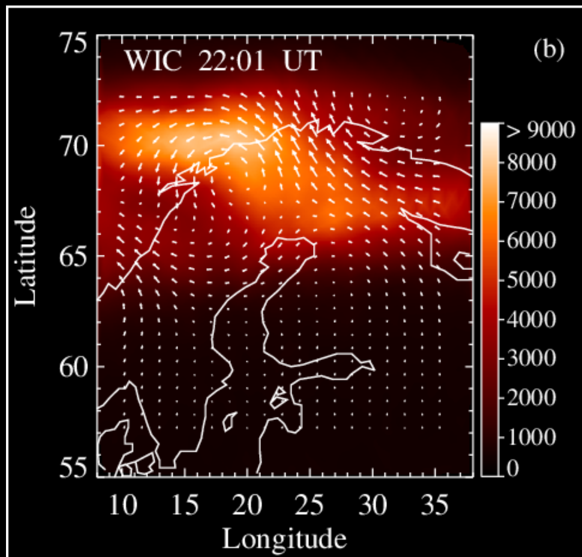

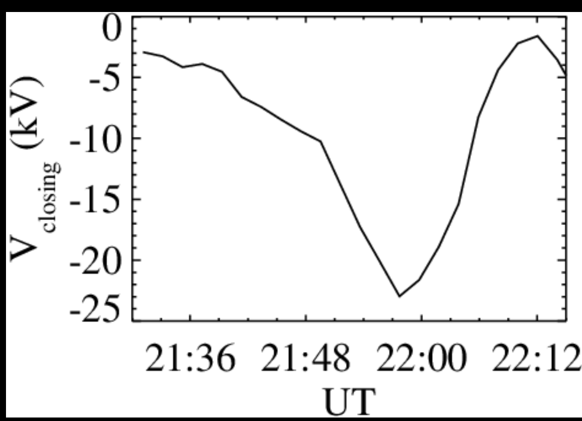

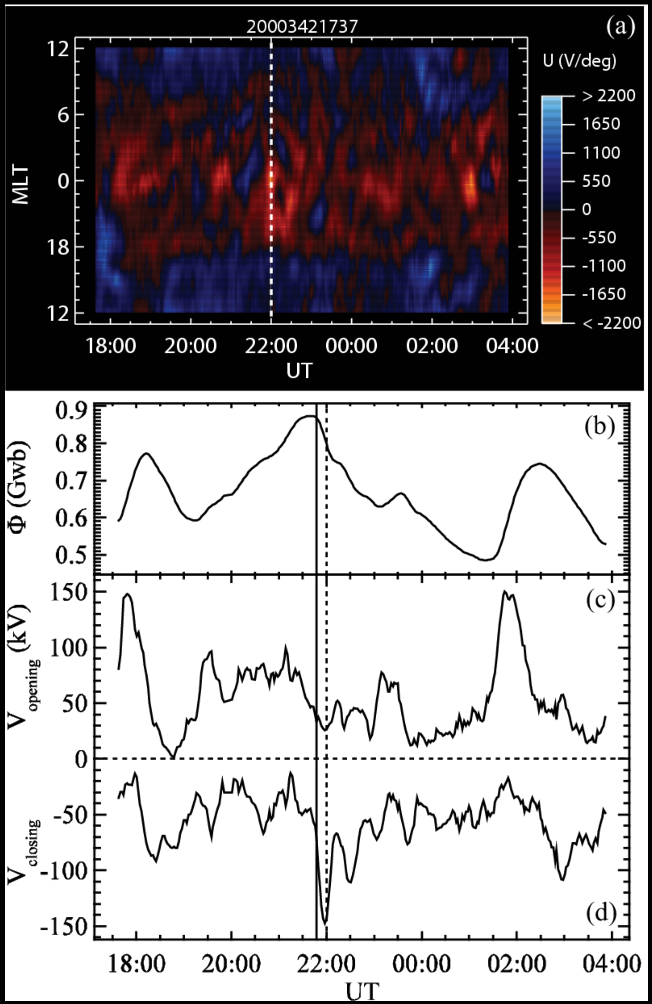

Comparison with other OCB identification techniques

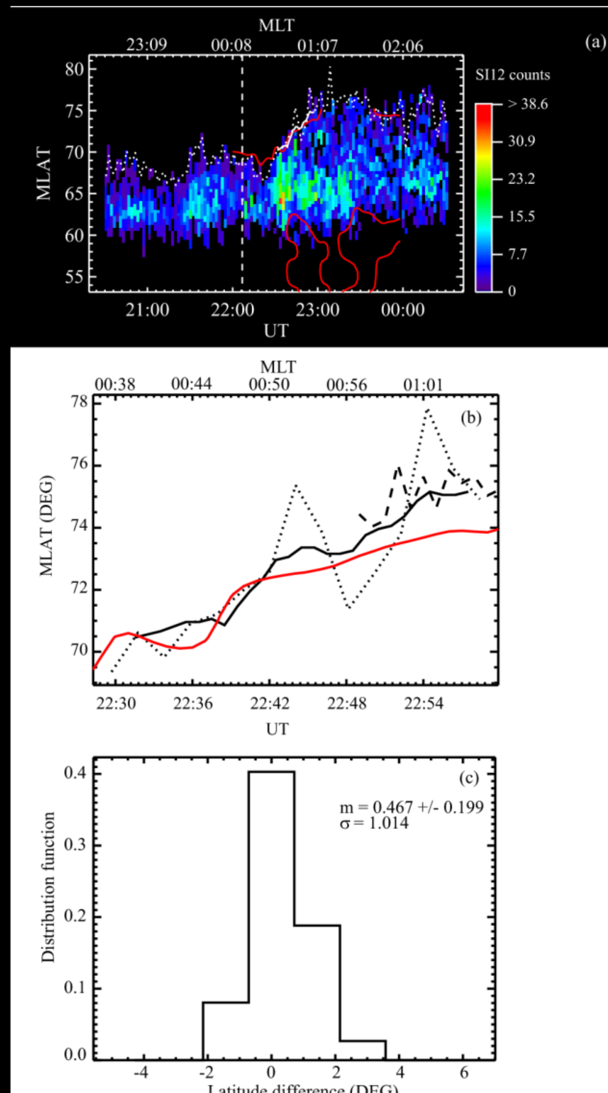

7 December 2000

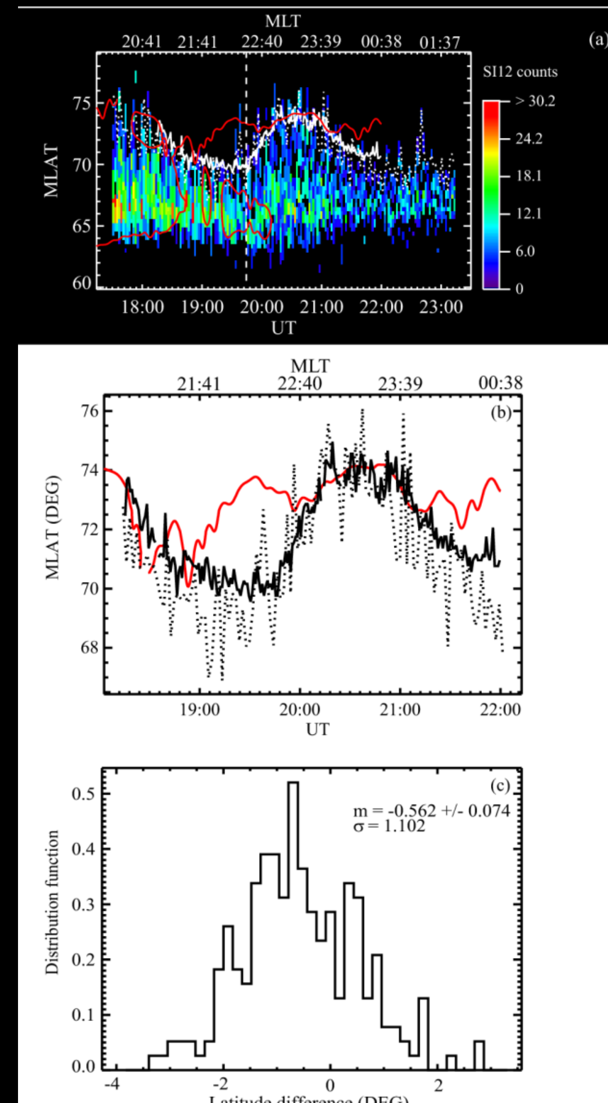

22 September 2001

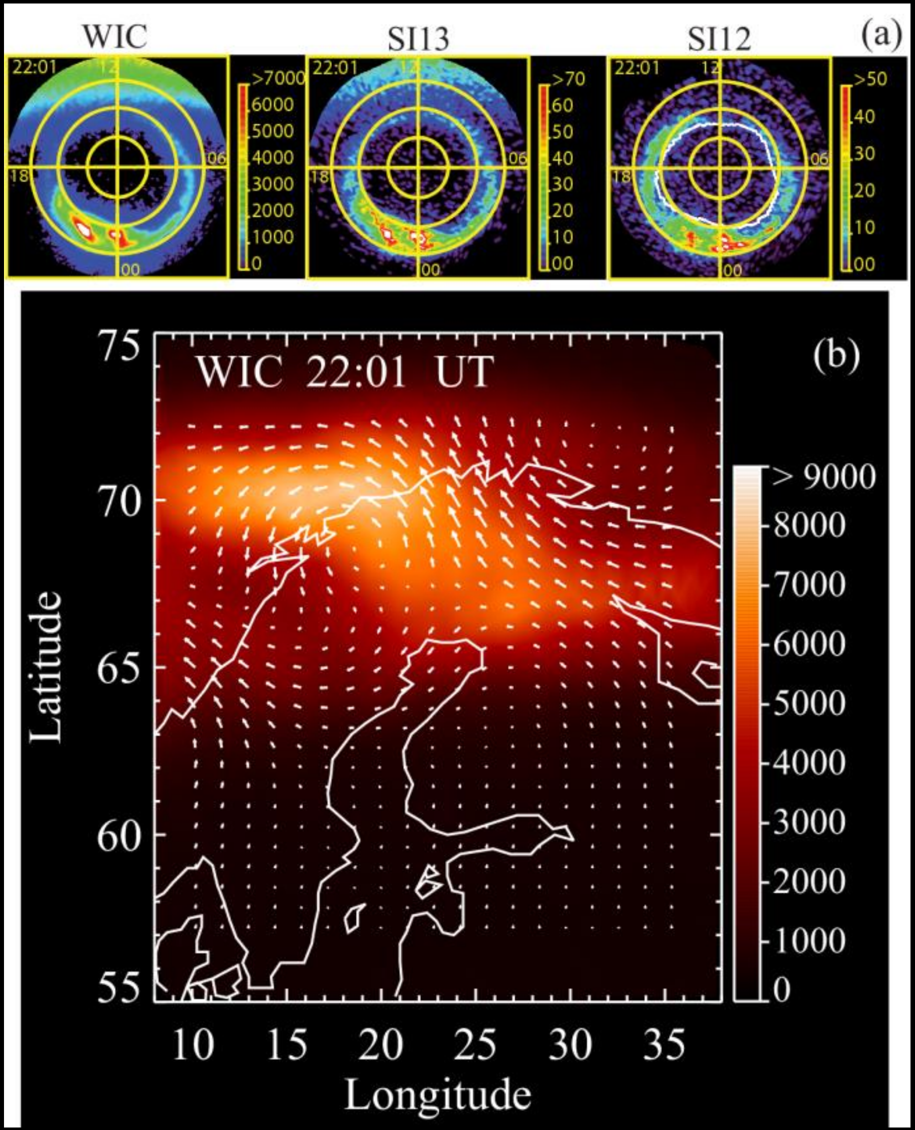
WIC
SI13
SI12
(a)
22:01
12
06
18
00
>7000
6000
5000
4000
3000
2000
1000
0
>70
60
50
40
30
20
10
00
>50
40
30
20
10
00
WIC 22:01 UT
(b)
Latitude
75
70
65
60
55
10
15
20
25
30
35
Longitude
> 9000
8000
7000
6000
5000
4000
3000
2000
1000
0

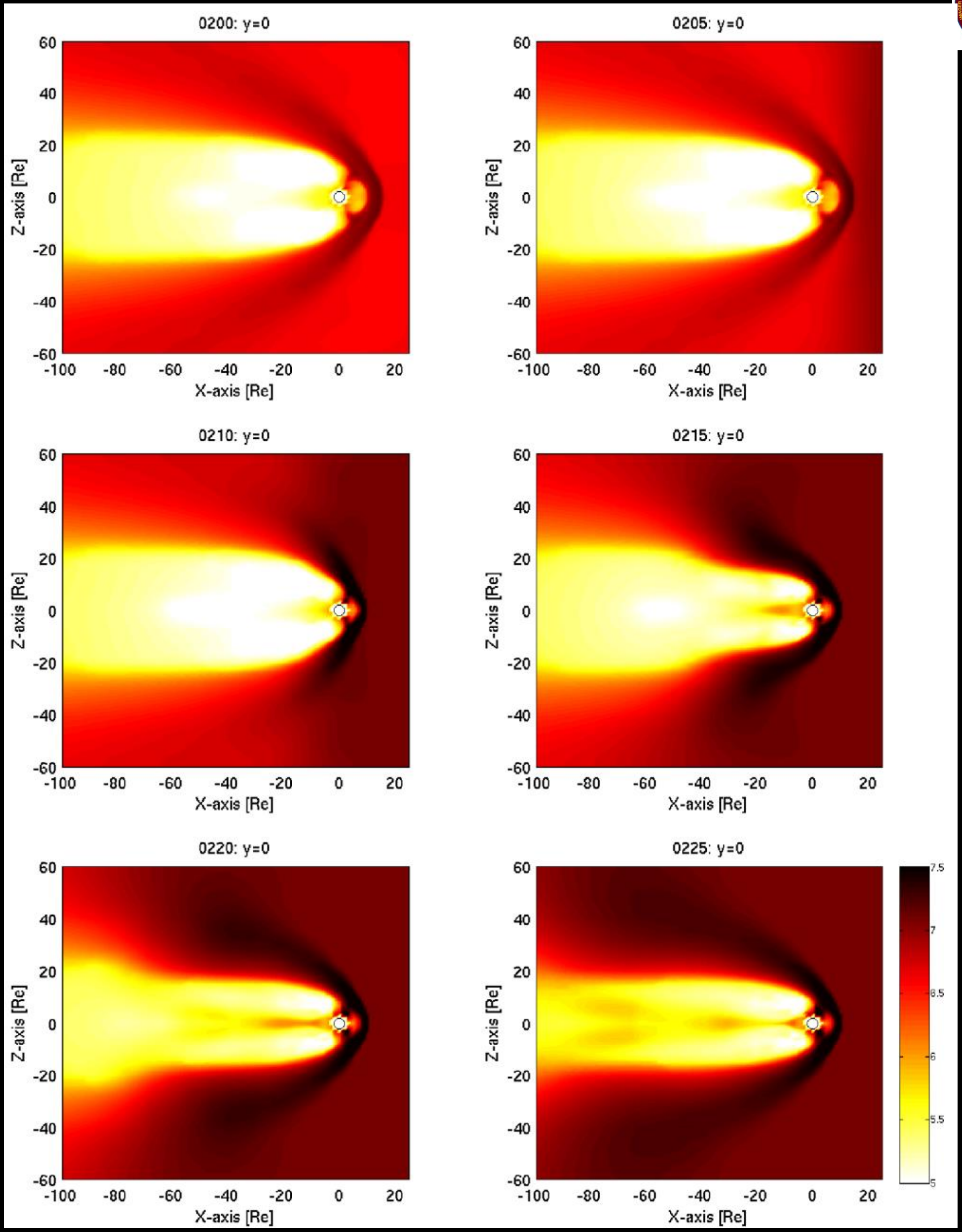
0200: y=0
0205: y=0
0210: y=0
0215: y=0
0220: y=0
0225: y=0
Z-axis [Re]
X-axis [Re]
7.5
7
6.5
6
5.5
5

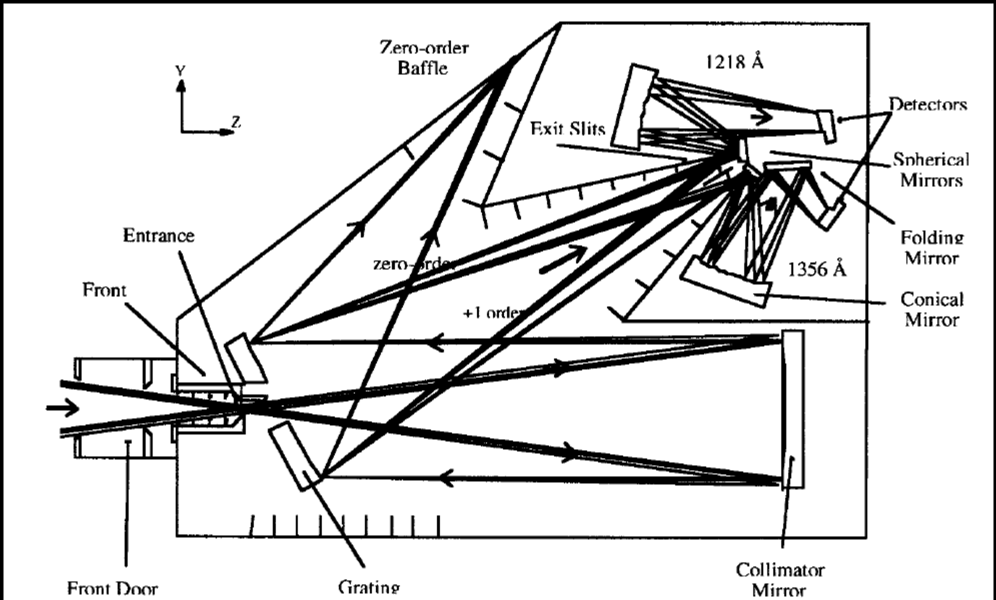

Figure 3. The IMAGE Spectrographic Imager schematic.

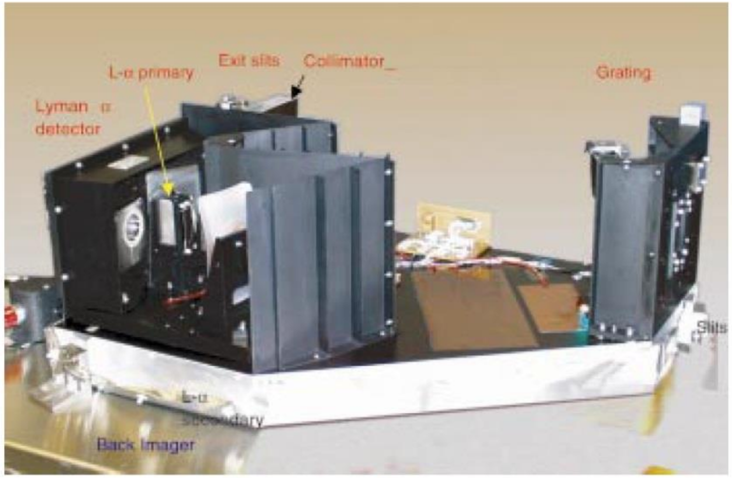

Figure 4. The Spectrographic Imager without its cover.